

Internal Wave Generation in the Equatorial Undercurrent

Dailin Wang

International Pacific Research Center, School of Ocean and Earth Science and Technology,
University of Hawaii at Manoa, Honolulu, Hawaii

Peter Müller

Department of Oceanography, School of Ocean and Earth Science and Technology, University of
Hawaii at Manoa, Honolulu, Hawaii

Abstract.

The generation of internal waves in the equatorial undercurrent is studied using a large-eddy simulation (LES) model. The model is forced with a constant easterly windstress and diurnal heating and cooling. Internal waves are generated with typical horizontal wavelengths of about 250 m, consistent with observations and comparable to the wavelengths of the most unstable modes from linear instability analysis. The internal waves exhibit a diurnal cycle below the boundary layer, or well below the mixed layer. The equatorial undercurrent (EUC) shear is crucial for the generation of these “long” internal waves. The range of diurnal variation of the wave energy (or equivalently, the isotherm displacement) is also consistent with observations. The wave energy is highly correlated with turbulence dissipation in the stratified regions of the boundary layer, in agreement with observations. The wave energy flux below the boundary layer has a maximum value of about 0.4 mW/m^2 near the core of the EUC. The wave energy flux into the deep ocean is about one order of magnitude smaller. The interaction of nighttime convection with the EUC does not contribute significantly to the internal wave field in the deep ocean.

1. Introduction

It has been well over a decade since the first observations of deep diurnal cycle turbulence at the equator [Gregg *et al.*, 1985; Moum and Caldwell, 1985]. Various mechanisms have been proposed for this deep-cycle turbulence, including Kelvin-Helmholtz instability of the mean and/or local shear and internal wave breaking in the high but stable shear environment. One of the characteristics of the deep-cycle turbulence is the existence of internal waves with typical wavelengths of a few hundred meters below the mixed layer [e.g., McPhaden and Peters, 1992; Lien *et al.*, 1996]. Two dimensional numerical studies [e.g., Skyllingstad and Denbo, 1994] also show the existence of such internal waves. The most unstable modes of the EUC system also have these wavelengths, as shown by the linear analyses of Sutherland [1996] and Sun *et al.* [1998]. The linear analyses require the mean shear to be unstable above a certain depth (in the mixed layer and/or in part of the stratified layer be-

low the mixed layer). The vertical wavelengths of the growing waves are, however, much larger than the region of dynamic instability. Sun *et al.* [1998] suggested that these internal waves play a critical role in the generation of the deep-cycle turbulence, although it cannot be deduced from linear analysis whether or not these waves develop into turbulence because of the lack of an active turbulent boundary layer and the infinitesimal growth assumptions.

In a recent study by Wang *et al.*, [1998], who used a large-eddy simulation (LES) model, the deep diurnal cycle of turbulence was qualitatively reproduced. This study suggests that local Kelvin-Helmholtz (K-H) instability is the major cause of the deep-cycle turbulence. It also suggests that the deep-cycle turbulence is a contiguous part of the boundary layer in the presence of the equatorial undercurrent (EUC). Since the model domain size of this study was not large enough to resolve the observed internal waves with wavelengths of a few hundred meters, the results of their study seem

to contradict the suggestion of *Sun et al.* [1998]. Further investigations are warranted of how these internal waves are generated and whether or not these internal waves have any effects on the deep-cycle turbulence.

In this study, we investigate the generation of long internal waves in the equatorial boundary layer using a large-eddy simulation (LES) model with a much larger domain than that used in *Wang et al.* [1998] so that internal waves with wavelengths of a few hundred meters can be resolved (for the remainder of this paper, we shall refer to these internal waves as “long internal waves”, to distinguish them from short internal waves, which can also be generated in the LES model). The advantage of a 3-D LES model over 2-D models and linear analyses is that both turbulence (large eddies) and internal waves are resolved simultaneously. Here we focus on the following questions:

Can long internal waves be generated from the interaction of diurnally cycling turbulence and the equatorial undercurrent shear?

What is the generation mechanism of these waves?

Do these waves carry a significant wave energy flux into the deep ocean?

The effects of these long internal waves on the deep-cycle turbulence itself will be discussed elsewhere.

The LES model and numerical experiments are described in section 2. Model results are presented in section 3 and some concluding remarks are made in section 4.

2. Model and Numerical Experiments

The LES model used in this study is based on a newer version [Sullivan *et al.*, 1996] of the LES model originally developed by Moeng [1984]. The model employs collocation Fourier method in the horizontal and second order finite difference in the vertical. Some of the large-scale flow terms typical of eastern Pacific conditions are also included: the equatorial undercurrent (EUC), zonal pressure gradient, upwelling, horizontal divergence, zonal temperature gradient, and mesoscale eddy forcing terms for the zonal momentum and the heat equations. The governing equations are

$$\mathbf{u}_t + \mathbf{u} \cdot \nabla \mathbf{u} = -\nabla p - \alpha \mathbf{g} T + \nabla \cdot \boldsymbol{\tau} + \mathbf{G}, \quad (1)$$

$$\nabla \cdot \mathbf{u} = 0, \quad (2)$$

$$T_t + \mathbf{u} \cdot \nabla T = \nabla \cdot \mathbf{q} + \frac{1}{C_p} \partial_z I(t, z) + H_T, \quad (3)$$

$$e_t + \mathbf{u} \cdot \nabla e + W e_z = \boldsymbol{\tau} : \nabla \mathbf{u} - \alpha g q_3 - \epsilon + \nabla \cdot 2\mathbf{K} \cdot \nabla e, \quad (4)$$

where $C_p = 4.1 \times 10^6 \text{ J m}^{-3} \text{ K}^{-1}$ is the specific heat of sea water per unit volume and $\alpha = 0.00027 \text{ K}^{-1}$ is the thermal expansion coefficient. The large scale terms G and H_T are given by

$$\begin{aligned} G_u &= -uU_x - vU_y - Wu_z - P_x + F_u, \\ G_v &= -uV_x - vV_y - Wv_z - P_y + F_v, \\ G_w &= -uW_x - vW_y - Ww_z + F_w, \end{aligned} \quad (5)$$

and

$$H_T = -u\hat{T}_x - v\hat{T}_y - WT_z + F_T, \quad (6)$$

where $\mathbf{F} = (\mathbf{F}_u, \mathbf{F}_v, \mathbf{F}_w)$ and F_T represent mesoscale eddy forcing that is not explicitly contained in the LES model. The variables in upper cases are prescribed. Further details of the model physics and subgrid scale parameterizations (SGS) are given in *Wang et al.* [1998, section 2 and appendices therein].

The model domain size for the present study is $640 \text{ m} \times 160 \text{ m} \times 270 \text{ m}$, with a resolution of $128 \times 32 \times 270$. In the zonal direction, this model domain size is four times that of the largest domain size used in *Wang et al.* [1998]. Ideally, the domain size in the meridional direction should also be 640 m, instead of 160 m as used here. The choice of the smaller domain size in the meridional direction size is purely based on the availability of computing resources. However, with 32 grid points in the meridional direction, the resolved large eddies within the boundary layer are still three dimensional. A 3-D configuration is required. We were unable to generate turbulence in a 2-D configuration without added random forcing at the surface. *Skyllingstad and Denbo* [1994] employed large amplitude (as much as 30% of the prescribed value) random surface forcing in their 2-D study, for as long as a 24-hour period, to facilitate spinup of 2-D large eddies.

The initial condition of the numerical experiment is obtained by repeating 16 times the $16 \times 16 \times 270$ resolution case in *Wang et al.* [1998, experiment I] at 3 p.m. of day five, with some small initial noise (with velocity variance of order $10^{-6} \text{ m}^2/\text{s}^2$) introduced to break the symmetry of the original solution. Without the noise, it would take a very long time for motions with scales larger than the small domain to develop (only possible because of machine truncation errors). The surface forcing are a constant zonal windstress of $\tau = -0.042 \text{ N/m}^2$, a constant cooling rate of $Q = -200 \text{ W/m}^2$, and a sinusoidal penetrative solar heating with noontime maximum insolation of 776 W/m^2 . The model is integrated forward for two days.

We also conducted a pure convection experiment to contrast its solution with that of the experiment de-

scribed above to gain insights into the generation mechanisms of internal waves. The convection experiment employs a domain size of $960 \text{ m} \times 320 \text{ m} \times 270 \text{ m}$, with a resolution of $192 \times 64 \times 270$.

3. Results

3.1. Diurnal Cycle of Internal Waves

The diurnal cycle of the boundary layer is caused by the diurnal solar heating. At night, when solar heating is absent, convection occurs because of surface cooling. The mixed layer deepens and turbulence grows. During the day, restratification of the surface layer due to intense solar heating suppresses convection and turbulence decays despite the windstress forcing. In this section we present evidence of the diurnal cycle of internal wave generation below the boundary layer.

Figure 1 shows a snapshot of vertical velocity in the $x - z$ plane typical of the early morning hours. The mixed layer has a depth of about 30 m. The boundary layer extends to about 80 m depth. The zonal scales of motions below the boundary layer are about 250 m. The vertical scales are on the order of 80-100 meters. Closer examination of the time evolution shows that these large scale features have upward phase propagation and are coherent over a large vertical extent. These large scale features can be traced upward into the boundary layer. For example, the positive vertical velocity region, centered at $x = 130 \text{ m}$, extends from 160 m to about 20 m, with zonal scales of about 80 m at the depth of 80 m. Similar features are also observed for the other two positive velocity regions, centered at 330 m and 550 m, respectively. We interpret these large scale upward propagating features as long internal waves. For internal waves upward phase propagation implies downward energy propagation.

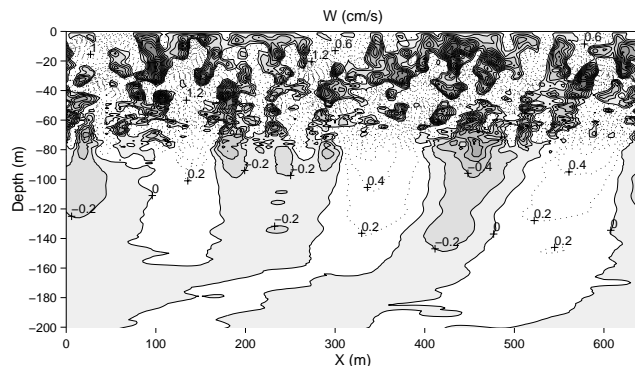


Figure 1. A zonal section of vertical velocity at 6 a.m. Regions with negative vertical velocities are shaded. Positive contours are indicated by dotted lines. The range of vertical velocity is about $[-3, 3]$ cm/s. Contour interval = 0.2 cm/s.

The horizontal and vertical scales of resolved motions above 40 m are a few tens of meters and exemplify convective turbulence (of course, if the resolution is still finer, smaller scale motions can also be resolved). The stratified region below 40 m but above 80 m shows somewhat smaller scales of motions, compared to the region above. This is because stratified turbulence tends to have smaller scales in more stable stratification. As described above, these small scales are modulated by the long internal waves extending upward into the boundary layer. Note that the small scale motions are absent in *Skyllingstad and Denbo's* [1994] 2-D simulation. However, long internal waves are still generated. We shall defer the discussion of the generation mechanism of these long internal waves to section 3.3.

We will next address the question whether or not internal waves below the turbulent boundary layer exhibit a diurnal cycle. First we define as a measure of nonlinearity the ratio γ of the rms perturbation temperature gradient to the mean temperature gradient

$$\gamma = \frac{\sqrt{\langle T_z'^2 \rangle}}{\langle T_z \rangle},$$

where triangle brackets denote horizontal averages. Above 80 m, γ tends to be larger than one (except during the daytime decay of turbulence in the mixed layer) and to be smaller than one below 80 m. Therefore, the motions above 80 m are more nonlinear, or more turbulence-like, and the motions below 80 m are more linear, or more wave-like (see also [Wang *et al.* 1998]). This behavior of γ is another indication that the large scale feature below 80 m are internal waves.

Figure 2 shows the normalized vertical velocity variance $\langle ww \rangle$ as a function of time and depth. The mixed layer depth, defined as the depth at which density differs from that of the surface by 0.01 kg/m^3 , is also shown (dashed line). The mixed layer depth varies from 5 m during the day to 30 m at night. The boundary layer depth, defined as the depth at which the momentum flux or heat flux becomes zero (or a small fraction of the corresponding surface fluxes), is different from that of the mixed layer depth. For example, in the early morning hours, the boundary layer depth is roughly 80 m, while the mixed layer is much shallower.

After sunset and above 80 m (i.e., in the turbulent region), the depth at which the vertical velocity variance is maximal increases with time, a characteristic of turbulent entrainment. It takes time for convective turbulence to reach deeper depths. The growth of turbulence is gradual. It takes many hours for turbulence to reach deeper depths. In contrast, below 80 m (or in the wave region), there is no apparent phase difference between different depths: maximal vertical velocity variance is

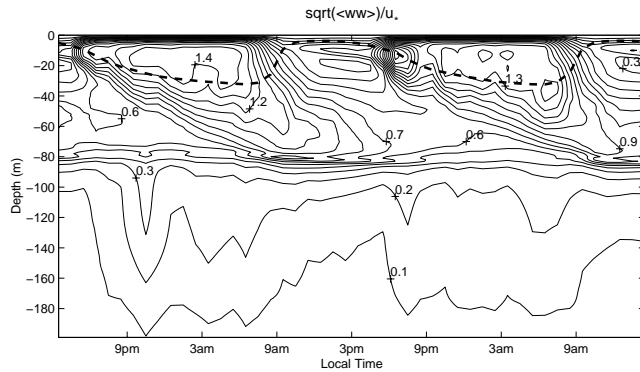


Figure 2. Vertical velocity variance, normalized by the surface friction velocity. The time axis covers two days, starting and ending 3 p.m. local time. The dashed line indicates the depth of the mixed layer, which is defined as the depth at which density differs from that of the surface by 0.01 kg/m^3 .

reached at the same time at all depths, such as the feature near 10 p.m. of the first diurnal cycle and near 8 p.m. of the second diurnal cycle. This is a characteristic of internal waves, of fast vertical propagation. The diurnal cycle of vertical velocity variance below 80 m thus indicates a diurnal cycle of internal wave activity below the boundary layer. In the 2-D study of *Skyllingsstad and Denbo* [1994] there are no separate regions of turbulence and waves. The rms of vertical velocity in their whole region resembles that of the wave region in this study.

3.2. Wave Energy

Observational studies often calculate the normalized displacement variance

$$P_e = N^2 \eta^2, \quad (7)$$

where $\eta^2 = \langle T'^2 \rangle / \langle T_z \rangle^2$. Figure 3 shows time series of P_e at 30, 60, 70, and 80 m. At 30 m and 80 m (solid line and dot-dashed line), P_e varies by a factor of about ten over a diurnal cycle, which is comparable to the observations of *Moum et al.* [1992]. At 60 m and 70 m, the diurnal variations of P_e are much smaller, only about a factor of two. This is small compared to observations. This discrepancy might be due to the fact that environmental conditions used in our model are not exactly comparable to the observations. In terms of gradient Richardson number Ri , a depth of 80 m in our study corresponds to a depth of about 50 m in *Moum et al.* [1992, Figure 7].

Observations also show a high degree of correlation between ρ_e and turbulence dissipation. Figure 4 shows this correlation coefficient from our numerical simulation. The correlation coefficient is small for the depth

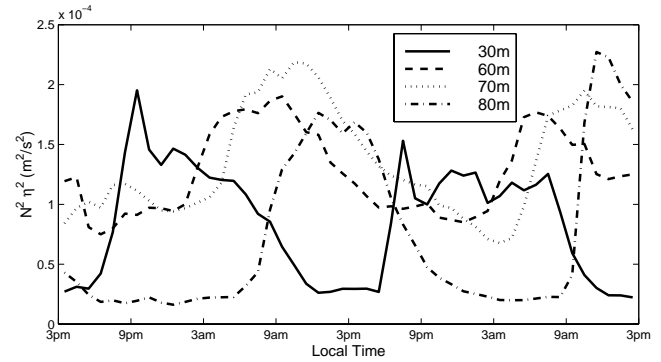


Figure 3. Time series of $N^2 \eta^2$ at 30, 60, 70, and 80 m.

range of 0-10 m, greater than 0.8 for the depth range 15-80 m, and then decreases towards deeper depths. This finding is also comparable to the observations of *Moum et al.* [1992], who found the correlation coefficient to be near 0.8 away from the surface and no significant correlation below the depth of 50 m, which is comparable to the depth of 80 m in our numerical study.

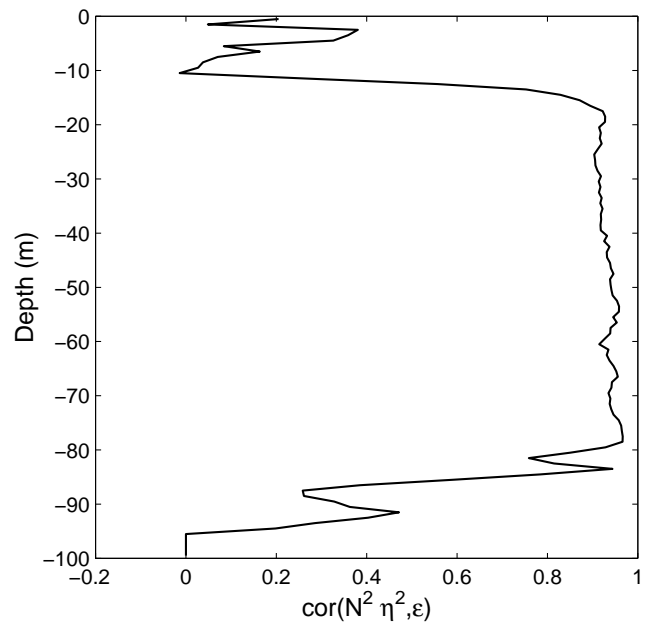


Figure 4. Correlation coefficient between $N^2 \eta^2$ and turbulence dissipation.

The displacement variance P_e defined by (7) is often referred to as internal wave energy in the literature [e.g., *Moum et al.* 1992; *Lien et al.* 1996]. P_e is indeed the total energy of internal waves if one assumes equipartition between potential and kinetic energy, which is the case for high frequency internal waves. Thus P_e represents the wave energy at depth below 80 m. This is not true in the stratified region above 80 m where

we also have turbulence. We have not attempted separating turbulence and waves in this region. *D'Asaro and Lien* [this volume] and *Lien et al. [1998]* suggest a method of separating turbulence and waves according to the Brunt-Väisälä (or buoyancy) frequency N . Motions with Lagrangian frequencies higher than N are considered turbulence while motions with frequencies below N are considered waves. Turbulent large eddies can also have time scales (eddy turnover times) longer than the buoyancy period, and that this distinction might not be fully adequate. We will explore the possible use of this method in diagnosing LES solutions in future studies.

3.3. Mechanisms of Wave Generation

In section 3.1, we showed that long internal waves are generated when the model domain was large enough. One immediate question that follows is whether such long internal waves can be generated without the presence of an equatorial undercurrent shear. To address this question, we conducted a pure convection experiment with the same initial stratification as that of the experiment with the EUC and with the same surface cooling rate of 200 W/m^2 . Figure 5 shows a typical zonal section of vertical velocity. There are internal waves below the boundary layer. The vertical and horizontal scales of these waves, however, are small compared to the case with the EUC shear (compare with Figure 1). The amplitudes of these waves are also much smaller. It is intriguing that the internal waves have smaller scales near the bottom of the boundary layer than well below the boundary layer. We do not yet have an explanation for this behavior. Comparison of the convection experiment and the experiment with the EUC demonstrates that the presence of the EUC shear is crucial for the generation of the long internal waves.

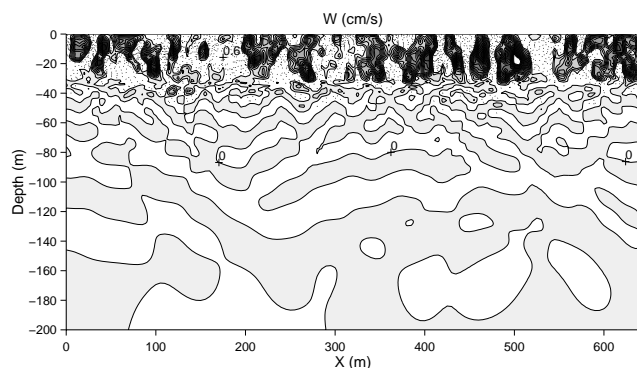


Figure 5. A zonal section of vertical velocity for pure convection experiment at time=210 min. Regions with negative vertical velocities are shaded. Positive contours are indicated by dotted lines. Contour interval=0.2 cm/s.

To investigate the role of the shear in the genera-

tion of long internal waves, Figure 6 shows the gradient Richardson number Ri at 6 a.m. and 6 p.m. At 6 a.m., Ri is near the critical value of $1/4$ for most part of the 0-50 m depth range. At 6 p.m., most of the water column is stable except near the surface, where nighttime convection has already commenced. We conclude that the diurnal cycle of the resolved long internal waves below the boundary layer in our model is a direct result of the diurnal cycle of mean shear instability inside the boundary layer.

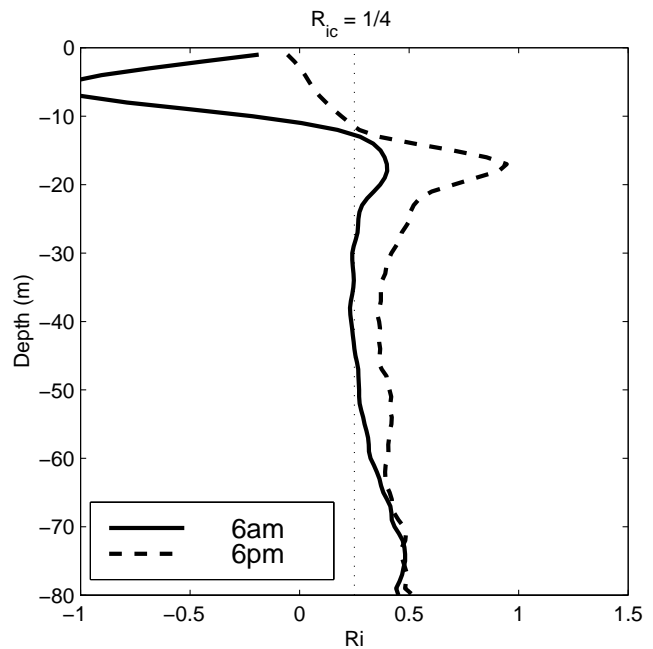


Figure 6. Gradient Richardson number Ri . The dotted line indicates critical Richardson number $Ri_c = 1/4$.

The fact that 2-D studies and linear analyses also show the generation of these long internal waves implies that turbulence convection is not a necessary condition for the generation of the long internal waves. As long as the mean shear is unstable, long internal waves tend to grow given the right scale of disturbances. We further speculate that long internal waves might also be generated due to local K-H instability, in a stable mean environment. Future studies are needed to test this hypothesis.

3.4. Wave Energy Flux into the Deep Ocean

Figure 7 shows a profile of the vertical energy flux $\langle pw \rangle$ at 6 a.m. Its divergence is a small term in the overall turbulent kinetic energy budget. Below 80 m the energy flux is interpreted as an internal wave energy flux. The flux peaks just below the boundary layer, around 110 m, with a value of 0.4 mWm^{-2} , and then decreases with depth. Only a flux of about 0.02 mWm^{-2}

leaves the domain towards the deep ocean. This flux is much smaller than the flux of 1 mWm^{-2} quoted or implied for wind forced and tidally generated internal waves (e.g., *Olbers* 1983). If the LES code correctly implements the radiation condition at the lower boundary of the model domain then we must conclude that internal waves generated by the interaction of nighttime convection with the EUC shear does not significantly contribute to the deep ocean internal wave field.

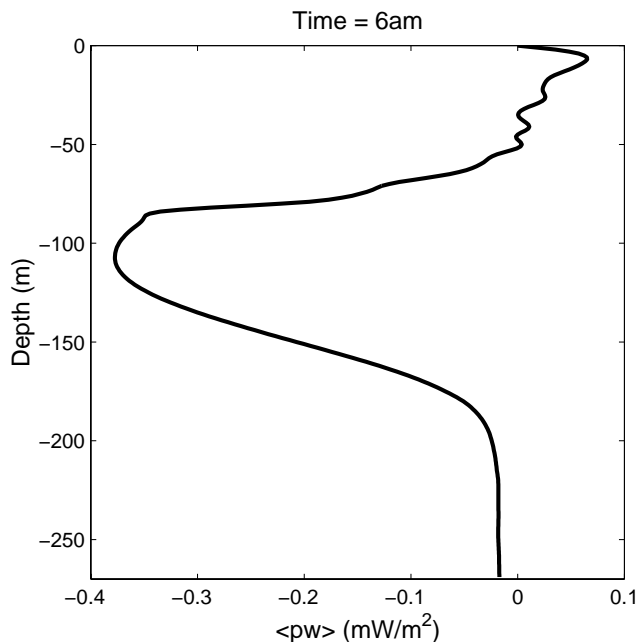


Figure 7. Wave energy flux $\langle pw \rangle$ at 6 a.m.

4. Conclusion

Internal wave generation in the equatorial undercurrent is investigated using a large eddy simulation model with a larger domain size than previous LES studies. It is found that internal waves with typical wavelengths of 250 m are generated as an integral part of the equatorial boundary layer. The equatorial undercurrent shear is crucial for the generation of these waves. The mean shear is more unstable during nighttime convection than during the daytime restratification when only the surface layer is dynamically unstable. This diurnal cycling of the mean shear causes a diurnal cycle in the internal wave energy.

The wave energy flux into the deep ocean is calculated to be of order 0.02 mW/m^2 , which is small compared to energy fluxes for wind and tidally generated internal waves.

We also found that the long internal waves have minor effects on the deep-cycle turbulence. A detailed

examination of this issue will appear elsewhere.

In this and other numerical studies, and also in observations, it is not always clear how to distinguish waves from turbulence and whether or not such a distinction even makes sense in a stratified environment. We ascribed motions within the mixed layer to turbulence and motions well below the boundary layer to waves but made no attempt to separate these components in the transitional layer, or entrainment layer, where turbulence is very intermittent. It is even questionable whether the LES models with resolutions of a few meters adequately resolve these intermittent motions.

Acknowledgments. Funding to D. Wang is provided by Frontier Research System for Global Change. D. Wang is grateful to Humio Mitsudera for his encouragement. This is SOEST contribution no. 4865.

References

- Gregg, M. C., H. Peters, J. C. Wesson, N. S. Oakey, and T. J. Shay, Intensive measurements of turbulence and shear in the equatorial undercurrent, *Nature*, 318, 140-144, 1985.
- Lien, R.-C., D. J. McPhaden, and M. C. Gregg, High-frequency internal waves at 0° , 140° W and their possible relationship to deep-cycle turbulence, *J. Phys. Oceanogr.*, 26, 581-600, 1996.
- Lien, R.-C., E. A. D'Asaro, and G. T. Dairiki, Lagrangian frequency spectra of vertical velocity and vorticity in high-Reynolds-number oceanic turbulence, *J. Fluid Mech.*, 362, 177-198.
- McPhaden, M. J., and H. Peters, Diurnal cycle of internal wave variation in the equatorial Pacific ocean: results from moored observations. *J. Phys. Oceanogr.*, 22, 1317-1329, 1992.
- Moeng, C. H., A large-eddy-simulation model for the study of planetary boundary-layer turbulence. *J. Atmos. Sci.*, 41, 2052-2062, 1984.
- Moum, J. N., and D. R. Caldwell, Local influences on the shear-flow turbulence in the equatorial ocean. *Science*, 230, 315-316, 1985.
- Moum, J. N., D. Hebert, C. A. Paulson, and D. R. Caldwell, Turbulence and internal waves at the equator. Part I: statistics from towed thermistors and a microstructure profiler, *J. Phys. Oceanogr.*, 22, 1330-1345, 1992.
- Olbers, D.J., Models of the oceanic internal wave field. *Rev. Geophys. Space Phys.*, 21,1567-1606, 1983.
- Skyllingstad, E. D., and D. W. Denbo, The role of internal gravity waves in the equatorial current system, *J. Phys. Oceanogr.*, 24, 2093-2110, 1994.
- Sullivan, P. P., J. C. McWilliams, and C-H Moeng, A grid nesting method for large-eddy simulation of planetary boundary-layer flows, *Boundary-Layer Meteorology*, 80, 167-202, 1996.
- Sun, C., W. D. Smyth, and J. N. Moum, Dynamic instability of stratified shear flow in the upper equatorial Pacific, *J. Geophys. Res.*, 103, 10,323-10,338, 1998.
- Sutherland, B. R., Dynamic excitation of internal gravity

waves in the equatorial oceans. *J. Phys. Oceanogr.*, 26, 2398-2419, 1996.

Wang, D., W. G. Large, and J. C. McWilliams, Large-eddy simulation of the equatorial ocean boundary layer: diurnal cycling, eddy viscosity, and horizontal rotation. *J. Geophys. Res.*, 101, 3649-3662, 1996.

Wang, D., J. C. McWilliams, and W. G. Large, Large-eddy simulation of the diurnal cycle of deep equatorial turbulence, *J. Phys. Oceanogr.*, 28, 129-148, 1998.

This preprint was prepared with AGU's L^AT_EX macros v4, with the extension package 'AGU++' by P. W. Daly, version 1.6a from 1999/05/21.